Stoichiometry and Conformation of Xanthan in Synergistic Gelation with Locust Bean Gum or Konjac Glucomannan: Evidence for Heterotypic Binding

F. M. Goycoolea, R. K. Richardson, and E. R. Morris*

Department of Food Research and Technology, Silsoe College, Cranfield University, Silsoe, Bedford MK45 4DT, England

M. J. Gidley

Colworth Laboratory, Unilever Research, Sharnbrook, Bedford MK44 1LQ, England

Received December 14, 1994; Revised Manuscript Received August 28, 1995[⊗]

ABSTRACT: Synergistic gels of xanthan or deacetylated xanthan (DX) with locust bean gum (LBG) or konjac glucomannan (KM) melt and set at ~60 °C, with no thermal hysteresis. Gelation occurs with the xanthan component in either its ordered or its disordered form and, with KM as cosynergist, is accompanied by large enthalpy changes (ΔH) in DSC. Gel modulus (G') and ΔH increase linearly with increasing ratio of KM:DX up to ~1:1, with little further change at higher ratios. Liquid-like character (tan δ) passes through a sharp minimum at about the same composition. Mixed gels of KM with unmodified xanthan show similar behavior, but the maximum value of ΔH is lower, and the proportion of KM required to achieve this maximum is higher. The heat changes (per gram of xanthan or DX) depend only on mixing ratio, not on total concentration, arguing strongly for stoichiometric binding rather than an exclusion mechanism. With LBG in place of KM, the sol−gel transition is much wider and gives no discernible peaks in DSC. The minimum in tan δ with varying composition, however, is still evident, again arguing for a binding process, and the moduli are higher (~3×). Gels incorporating KM show evidence of structural rearrangement after their initial formation (maxima in the temperature dependence of G''; shoulders in tan δ and in DSC); no such effects are seen for LBG. In the light of previous X-ray diffraction studies in the condensed phase, it is suggested that initial gelation involves heterotypic junctions between xanthan or DX and KM or LBG, with both components in a 2_1 conformation, but that junctions involving KM convert to a more compact 6-fold arrangement at lower temperature.

Introduction

The exopolysaccharide from *Xanthomonas campestris* is produced commercially as xanthan gum.[1] The xanthan molecule has a linear cellulosic backbone solubilized by charged trisaccharide side chains attached at O(3) of alternate glucose residues, to give a pentasaccharide repeat unit.[2,3] The side chains have the structure β-D-Man*p*-(1→4)-β-D-GlcA*p*-(1→2)-α-D-Man*p*-(1→ with variable, nonstoichiometric substitution by *O*-acetate at C(6) of the inner mannose and 4,6-linked pyruvate ketal groups on terminal mannose residues.

At high temperature and low ionic strength, xanthan exists in solution as a disordered coil. On cooling and/or addition of salt, however, it undergoes a cooperative conformational transition to a rigid, ordered structure. The transition is fully reversible with no detectable thermal hysteresis and has been monitored by a variety of physical techniques,[4−10] including optical rotation, circular dichroism, differential scanning calorimetry, viscometry, light scattering, and loss of detectable signal in high-resolution NMR. As found for other polyelectrolytes, adoption of the ordered structure is facilitated by increasing ionic strength, with consequent increase in the midpoint temperature (T_m) of the conformational transition. Removal of pyruvate substituents also raises T_m, by reducing electrostatic repulsion between chain segments. Acetate substituents, however, appear to contribute to the stability of the ordered structure,[11] and their removal lowers T_m.

Despite numerous investigations since the conformational transition of xanthan was first reported,[4] the nature of the ordered structure remains controversial. X-ray fiber diffraction patterns from oriented specimens in the condensed phase are equally consistent with two contending models: a single-stranded 5-fold helix stabilized by ordered packing of side chains along the polymer backbone[12] and a coaxial double helix,[13] with the participating strands having essentially the same geometry as in the single-helix model. Arguments in favor of both models have been put forward from solution studies.

Evidence for a double helix has come predominantly from light scattering[14−16] and, in particular, from measurements[16] of mass per unit length under different solvent conditions. The main evidence for a single-stranded structure is that the disorder−order transition follows first-order kinetics[8] and, in the absence of cations that are known to promote aggregation, can occur with no change in molecular weight.[7−9] Both of these observations would, however, be consistent with a double-helix structure incorporating some unusual feature that prevents complete separation of the constituent strands at high temperature. Possibilities would include a covalent linkage between the chains or consecutive runs of missing side chains, allowing stable association as in cellulose. There is, however, no experimental evidence of any such structural features.

Irrespective of the detailed geometry of the ordered structure, there is general agreement that its presence can generate unusual rheological properties.[17] At concentrations above ~0.3% w/v, solutions of commercial xanthan, although free-flowing, have obvious gel-like character and, in particular, will stabilize emulsions or hold small particles in suspension over long periods of time. In small-deformation oscillatory measurements,[18]

* Author for correspondence.

[⊗] Abstract published in *Advance ACS Abstracts,* November 1, 1995.

0024-9297/95/2228-8308$09.00/0

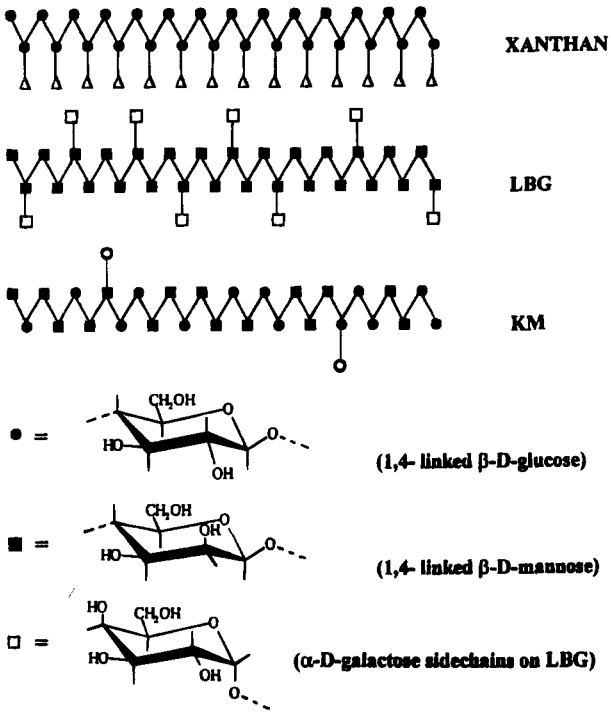

Figure 1. Primary structures of xanthan, locust bean gum (LBG), and konjac mannan (KM), shown schematically with the polymer backbones in the 2_1 chain conformation.

elastic response (storage modulus, G') substantially exceeds viscous flow (loss modulus, G''), and both moduli show only limited variation with frequency, as in conventional gels. At higher deformations, the network breaks, giving rise to large "stress overshoot" effects in start-shear experiments[19] and allowing the solution to flow.

These "weak-gel" properties are attributed to tenuous association of ordered chains and are sensitive to ionic environment. Studies of the same xanthan sample in different salt forms[20] showed a decrease in gel-like character through the series $Ca^{2+} > K^+ > Na^+$. Indeed with Na^+ as sole counterion, the solution properties of xanthan are close to those of disordered polysaccharides.[21] Commercial preparations,[1] however, normally have K^+ as the predominant counterion and also have a significant content of Ca^{2+}.

Although self-association of xanthan is limited to generation of "weak-gel" character in solution, the polymer will form true gels when mixed with certain plant polysaccharides,[22] notably locust bean gum (LBG) and konjac glucomannan, which is commonly known by the simpler name of konjac mannan (KM). Like xanthan, these materials have a linear backbone of hexapyranose sugars linked through equatorial bonds at positions 1 and 4 (Figure 1). In the solid state, both adopt an extended, ribbon-like, 2_1 conformation[23,24] similar to that of cellulose.[25]

Konjac mannan[26] is obtained from the tubers of *Amorphophallus konjac* and related species. The polymer backbone contains both β-D-mannose and β-D-glucose residues, in the approximate ratio 2:1, with no long blocks of either type. Solubility is conferred by *O*-acetyl substituents on a proportion (~5−10%) of the constituent sugars. Deacetylation (by alkaline hydrolysis) is sufficient to allow the chains to associate into a gel network.

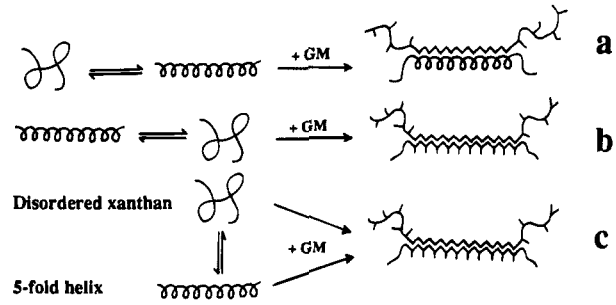

Figure 2. Proposed interpretations of the interaction of xanthan with galactomannan or glucomannan chains (GM): (a) "Unilever" model; (b) "Norwich" model; (c) proposal from the present work. The structures shown are highly schematic and are not intended to exclude the possibility of larger heterotypic assemblies.

The backbone residues in LBG (obtained from the seed endosperm of *Ceratonia siliqua*) are exclusively β-D-mannose, but the polymer is solubilized by α-D-galactose attached as irregularly spaced single-sugar side chains at O(6) of a proportion of the mannose residues.[22] The ratio of mannose to galactose (*M*/*G*) is typically ~3.5. Galactomannans with different contents of galactose occur in other leguminous species and include tara gum ($M/G \approx 2.7-3.0$) from *Caesalpinia spinosa* and guar gum ($M/G \approx 1.55$) from *Cyamopsis tetragonolobus*, both of which are produced commercially. Unsubstituted mannan is totally insoluble in water (although it can be dissolved in strong alkali) and the solubility of the galactomannans decreases with decreasing galactose content. Studies using rigorously purified enzymes to probe the distribution of galactose along the polymer backbone[27-29] indicate that sequences with more than six consecutive unsubstituted mannose residues are required to form stable intermolecular associations when galactomannan solutions are frozen and thawed.[29]

The ability of galactomannans to form synergistic gels with xanthan also increases with decreasing galactose content, prompting an early suggestion[6] from Unilever's Colworth Laboratory (Sharnbrook, Bedford, UK) that the gel network is formed by attachment of unsubstituted regions of the mannan backbone to the surface of the xanthan 5-fold helix (Figure 2a). In subsequent publications, this proposal was extended to sequences devoid of galactose along one side of the mannan chain in the 2-fold conformation[27,28] and to similar attachment of konjac glucomannan to the xanthan helix.[30]

More recently, however, it has been suggested[31-34] by workers in the Institute of Food Research, Norwich, UK, that attachment of mannan or glucomannan occurs only when the xanthan chain is in the disordered state and that the resulting heterotypic junctions involve direct binding of the plant polysaccharide to the cellulosic backbone of the xanthan molecule in an extended conformation rather than to the 5-fold helix (Figure 2b). This proposal is based on two main lines of evidence. (i) Solutions mixed under conditions where the xanthan helix is already present (low temperature and/or high concentration of counterions, particularly Ca^{2+}) remain fluid but give a cohesive gel after heating and recooling from a temperature at which xanthan is converted to the disordered form. (ii) X-ray diffraction from oriented specimens of xanthan with galactomannans or with KM gives intensities that do not appear in the diffraction patterns of either component in isolation.

For brevity, these two proposals will be referred to as, respectively, the "Unilever" model and the "Norwich"

model. A third proposal, by Tako, invokes noncovalent bonding between specific groups on galactomannan molecules and on the xanthan side chains.[35,36] This model, however, appears to have little basis in experimental evidence and incorporates some implausible features (such as the methyl groups of acetyl substituents participating in hydrogen bonding).

All three proposals discussed so far involve some form of direct binding between the constituent polysaccharides. It is, however, well established that apparent "synergistic" interactions between different polymers can arise from thermodynamic incompatibility,[37] either by phase separation (which raises the effective concentration of both components) or by exclusion effects promoting self-association within a single phase. Indeed an early report of formation of mixed gels between xanthan and LBG[38] described the phenomenon as a "useful incompatibility".

So far the most compelling evidence for direct binding is that (partially depolymerized) LBG has been observed to coelute with xanthan in gel permeation chromatography of mixed solutions.[39] An alternative route to distinguishing between binding and exclusion, however, is to examine the effect of the relative and absolute concentrations of the two components on the extent of interaction. Exclusion effects will normally become increasingly apparent as the concentration of either or both components is raised. Direct binding, by contrast, would be expected to involve some optimum ratio of the two polymers, largely independent of their total concentration.

One aim of the present investigation was to demonstrate that the synergistic interactions of xanthan do indeed display the stoichiometric relationships anticipated for a binding process. The second goal was to explore the validity of the "Unilever" and "Norwich" models by studying the temperature course of formation and melting of synergistic gels in relation to that of the xanthan disorder–order transition. The investigations were carried out using the lowest polymer concentrations at which reliable measurements could be obtained, to minimize the influence of nonspecific exclusion effects. A preliminary account of some aspects of the work has been published elsewhere.[40]

Experimental Section

All chemicals were AnalaR grade from BDH. Distilled deionized water was used throughout. A sample of konjac glucomannan from Senn Chemicals AG was kindly supplied by Dr. V. J. Morris (Institute of Food Research, Norwich, UK) and was from the same batch as the material used in the X-ray diffraction studies of Brownsey *et al.*[33] The powder was allowed to swell overnight in water (at ~2% w/v) and was dissolved by autoclaving for 20 min at 120 °C. Locust bean gum (Meypro fleur M-175 from Meyhall) was dissolved in the same way, but with initial dispersion in water in place of the preswelling step. Both solutions were clarified by centrifugation. Xanthan (Keltrol T; Kelco Division of Merck & Co. Inc.) was dissolved (at ~1% w/v) by gentle stirring (~4 h) at ambient temperature, yielding a clear solution. Deacetylated xanthan (DX) was prepared from Keltrol T by hydrolysis with NaOH (125 mM; 6 h at 45 °C under nitrogen) and was neutralized with HCl. All four preparations (KM, LBG, xanthan, and DX) were dialyzed extensively against water (four changes over 48 h), and the concentrations of the resulting stock solutions were determined by freeze-drying weighed aliquots. Solutions for physical studies were then dialyzed together against four changes of the appropriate salt solution (10 or 30 mM KCl), to eliminate changes in ionic environment on mixing. The samples were weighed before and after dialysis, and allowance was made for any changes in volume when calculating polymer concentrations. The final dialysate was used for all subsequent dilutions.

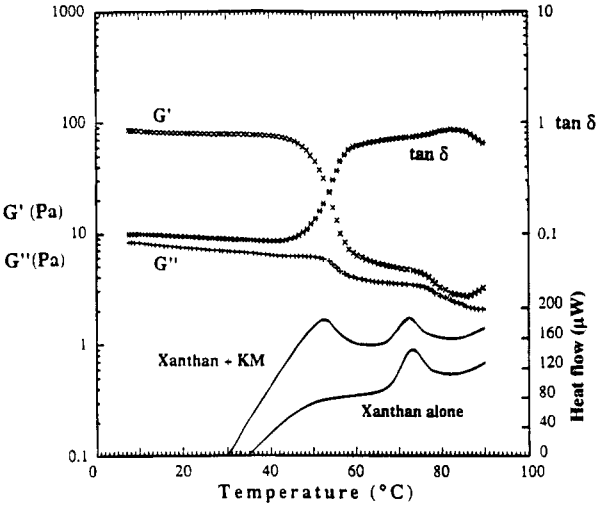

Figure 3. Lower traces: DSC cooling scans (0.2 deg/min) for xanthan (0.32% w/v in 30 mM KCl), alone, and in the presence of KM (0.24% w/v). Upper traces: variation of G', G'', and tan δ (10 rad s^{-1}; 2% strain) on cooling (1 deg/min) for the xanthan/KM mixed system; virtually identical curves were obtained on reheating.

Rheological measurements were made using cone and plate geometry (5 cm diameter; 0.05 rad cone angle) on a sensitive prototype rheometer designed and constructed by one of us (R.K.R.). Temperature was controlled by a circulating water bath and measured by a thermocouple in direct contact with the stationary element. Differential scanning calorimetry (DSC) measurements were made using a Seteram microcalorimeter. The appropriate dialysate was used as thermal reference, and sample and reference pans were balanced to within 0.1 mg.

Results

Xanthan in 30 mM KCl ($T_m > T_g$). Figure 3 shows DSC cooling scans for xanthan (0.32% w/v) in 30 mM KCl, alone, and in the presence of KM (0.24% w/v). Conformational ordering of xanthan alone gives an exotherm with a midpoint temperature of $T_m \approx 73$ °C and a transition enthalpy of $\Delta H \approx 4.4$ J g^{-1}. The same transition is evident with KM present but is then followed by a second, somewhat larger, exotherm at lower temperature. The figure also shows the changes in rheology of the mixed system on cooling, as monitored by low-amplitude oscillatory measurements (10 rad s^{-1}; 2% strain) of G', G'', and tan δ (the ratio of G''/G'). The xanthan disorder–order transition is accompanied by a small increase in rigidity (G'), with a much larger increase over the temperature range of the second transition in DSC. Visual inspection showed that this second process corresponds to formation of a self-supporting gel network. Both regions of increase in G' are accompanied by smaller increases in G''.

The temperature at the onset of the gelation process (the gelling temperature, T_g) is ~60 °C, and coincides closely with the onset of the second exotherm in DSC. Comparison with the DSC trace for xanthan alone indicates complete conformational ordering of the xanthan component at this temperature. This is, of course, inconsistent with the necessary involvement of disordered xanthan in synergistic gelation, as postulated in the "Norwich" model, but agrees well with the concept of binding to the xanthan helix, as in the "Unilever" model.

The changes in G', G'', and tan δ observed on reheating were closely superimposable on the cooling

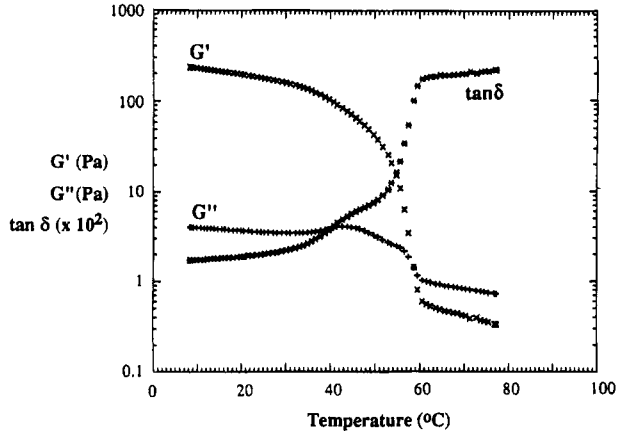

Figure 4. Temperature dependence of G', G'', and tan δ (10 rad s^{-1}; 2% strain) for deacetylated xanthan (0.32% w/v in 10 mM KCl) in combination with KM (0.24% w/v).

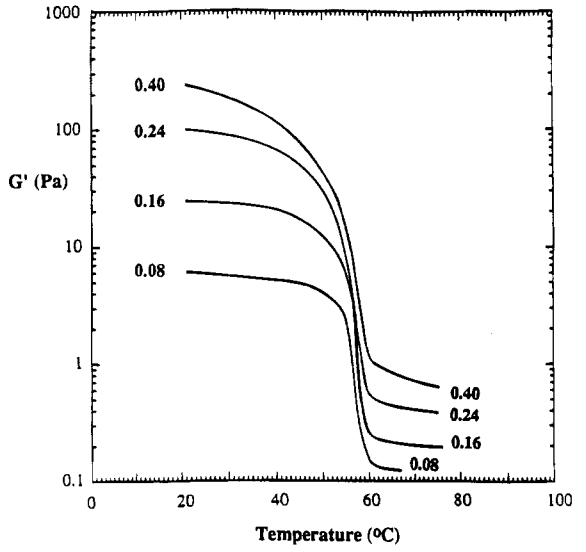

Figure 5. Temperature dependence of G' (10 rad s^{-1}; 2% strain) for KM (0.24% w/v in 10 mM KCl) in the presence of DX at the concentrations (% w/v) shown beside the individual traces.

curves shown in Figure 3 (i.e., with no detectable thermal hysteresis). The DSC heating scans were also closely similar to the corresponding cooling scans but, as discussed in detail later, were offset to slightly higher temperature because of finite rates of heat transfer ("thermal lag") in the calorimeter.

Deacetylated Xanthan in 10 mM KCl ($T_m < T_g$). In the experiments described so far, conformational ordering of xanthan occurred at a temperature well above the onset of synergistic gelation. The aim of the studies reported now was to explore the effect of displacing the conformational transition to much lower temperature. This was achieved by reducing the KCl concentration to 10 mM and by using deacetylated xanthan (DX) in place of the unmodified polymer.

In the first series of experiments carried out under these conditions, the concentration of KM was held constant at 0.24% w/v and DX concentration was varied between 0.08 and 0.40% w/v. Figure 4 shows the rheological changes observed on cooling for the same polymer concentrations as in Figure 3. Despite the 3-fold reduction in KCl concentration and the absence of acetate substituents on the xanthan, the temperature at the onset of gelation (as characterized by the steep increase in G') is unchanged ($T_g \approx 60$ °C). There is also

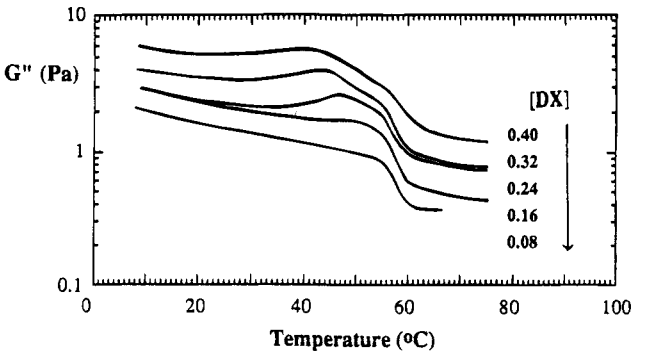

Figure 6. Temperature dependence of G'' (10 rad s^{-1}; 2% strain) for KM (0.24% w/v in 10 mM KCl) in the presence of DX at the concentrations (% w/v) shown.

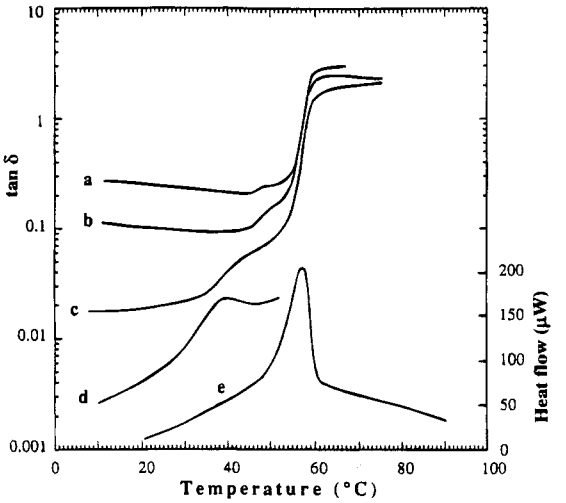

Figure 7. Traces a–c show the temperature dependence of tan δ (10 rad s^{-1}; 2% strain) for KM (0.24% w/v in 10 mM KCl) in the presence of DX at concentrations of, respectively, 0.08, 0.16, and 0.32% w/v. Traces d and e are DSC cooling scans (0.2 deg/min) for, respectively, 0.5% w/v DX in 10 mM KCl and a KM/DX mixture at the same concentrations as in (c).

clear evidence of a second process at lower temperature, giving a shoulder in the temperature dependence of tan δ and a maximum in G''. As found for unmodified xanthan at higher ionic strength, the traces obtained on reheating were virtually identical to those recorded on cooling.

Figures 5–7 show the temperature dependence of, respectively, G', G'', and tan δ for other concentrations of DX. To avoid confusing clutter, the figures include only selected, representative traces. Decreasing concentration of DX causes a progressive reduction in G', as would be expected, but has no effect on T_g (Figure 5). The maximum in G'' (Figure 6) is most clearly evident when the two polymers are present in equal amounts (i.e., at 0.24% DX); it becomes less apparent at higher concentrations of DX, and undetectable at the lowest concentration studied (0.08% w/v).

As illustrated in Figure 7, DSC scans for the KM/DX mixtures show a single transition coincident with the gelation process. Conformational ordering of DX alone under the same ionic conditions also gives a single transition, but at substantially lower temperature ($T_m \approx 39$ °C). It is evident, therefore, the gel formation in these systems occurs with the xanthan component in the disordered state, which is entirely consistent with the "Norwich" model but contradicts the earlier "Unilever" model.

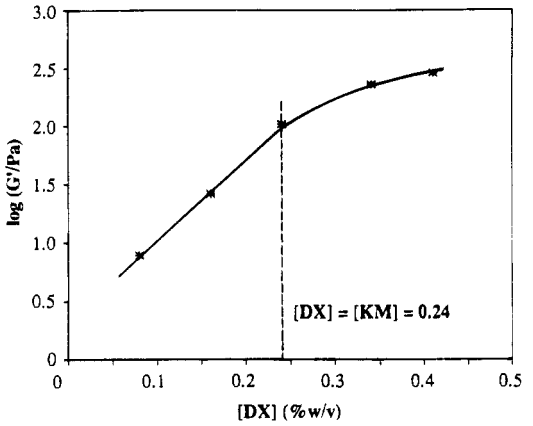

Figure 8. Variation of G' (10 rad s^{-1}; 2% strain; 10 °C) with concentration of DX in mixed gels with KM (0.24% w/v in 10 mM KCl).

At low concentrations of DX (i.e., when KM is present in excess), the shoulder in the temperature dependence of tan δ (Figure 7) remains close to the main gelling transition. At higher concentrations, however, the shoulder broadens into the temperature range of the disorder–order transition observed for DX alone. The maximum in G'' (Figure 6) shows a similar shift to lower temperature with increasing concentration of DX. A possible interpretation of this behavior is that there are two processes involved: some form of structural rearrangement at a temperature slightly below T_g, followed, at lower temperature, by conformational ordering of surplus DX when present in excess.

Figure 8 shows the composition dependence of gel rigidity (G') measured on completion of the cooling scans illustrated in Figure 5. Log G' increases linearly with DX concentration until the two polymers are present in equal amounts; beyond this point, log G' continues to increase, but with a lower concentration dependence. Detailed interpretation, however, is complicated by the possible contribution to overall modulus from the "weak-gel" properties of the xanthan component alone. A converse series of experiments was therefore carried out, in which the DX concentration was held constant (at 0.1% w/v in 10 mM KCl) and the KM concentration was varied between 0.01 and 0.60% w/v.

Figure 9 illustrates the temperature dependence of G' and G'' for these mixtures. As found in the previous experiments, T_g is unaffected by composition, remaining constant at ~60 °C. As shown in Figure 10, the final values of G' at low temperature increase steeply with increasing concentration of KM until the two polymers are present in roughly equal amounts (KM/DX $\approx$ 0.7) and then remain essentially constant at higher concentrations of KM.

As in the previous series of experiments (Figure 6), the maximum in the temperature dependence of G'' becomes most apparent (Figure 9b) when the polymers are present in equal proportions (i.e., at 0.1% w/v KM) and gradually disappears as the KM concentration is raised or lowered. Similar well-defined maxima are evident (Figure 11) for mixtures containing equal amounts of KM and DX at higher concentrations of the two components (0.24 and 0.40% w/v). As illustrated in Figure 12, DSC scans for mixtures incorporating comparable amounts of the two components showed indications of a slight shoulder on the low-temperature side of the main peak, roughly coincident with the maxima in G'' and the accompanying shoulder in tan δ. At the very low concentrations used for the rheological studies (0.1% w/v DX), the shoulder in DSC was barely discernible. Higher concentrations (0.4% w/v DX), however, gave a very obvious shoulder at KM concentrations equal to, or higher than, that of the DX component (Figure 13).

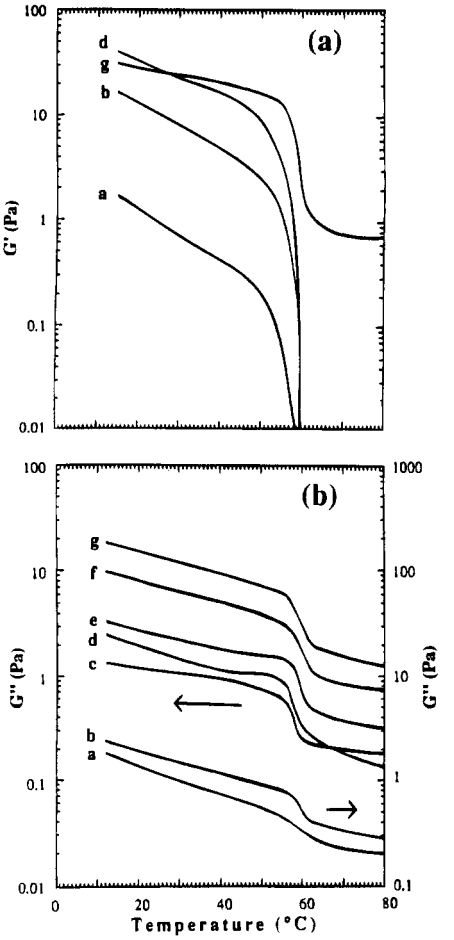

Figure 9. Temperature dependence of (a) G' and (b) G'' (10 rad s^{-1}; 2% strain) for DX (0.1% w/v in 10 mM KCl) in combination with KM concentrations (% w/v) of (a) 0.01, (b) 0.03, (c) 0.06, (d) 0.10, (e) 0.20, (f) 0.40, and (g) 0.60. The traces for G'' at the two lowest concentrations of KM (a and b) have been displaced downward by 1 decade to avoid overlap with those for the next highest concentrations (c and d); the absolute values of G'' for (b) are close to those for (d).

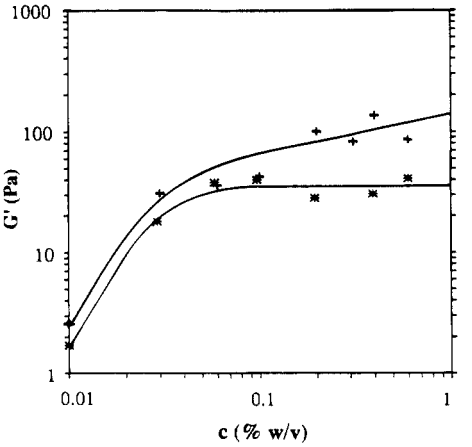

Figure 10. Variation of G' (10 rad s^{-1}; 2% strain; 10 °C) with concentration (c) of KM (*) or LBG (+) in mixed gels with DX (0.1% w/v in 10 mM KCl).

Figure 14 shows mechanical spectra recorded for DX/KM mixtures on completion of the cooling scans illustrated in Figure 9, in comparison with the spectrum

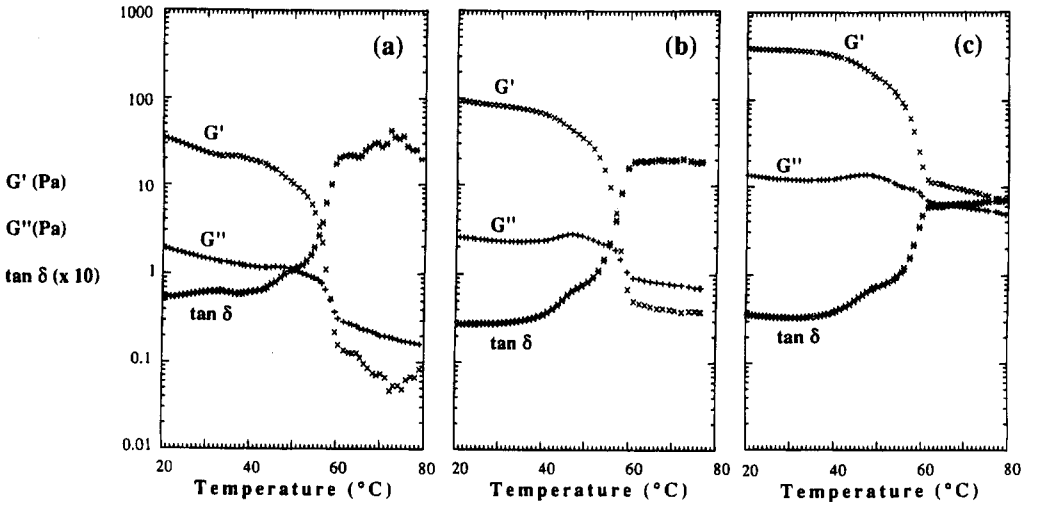

Figure 11. Temperature dependence of G', G'', and tan δ (10 rad s^{-1}; 2% strain) for DX/KM mixtures incorporating equal amounts of the two polymers at concentrations (% w/v in 10 mM KCl) of (a) 0.10, (b) 0.24, and (c) 0.40.

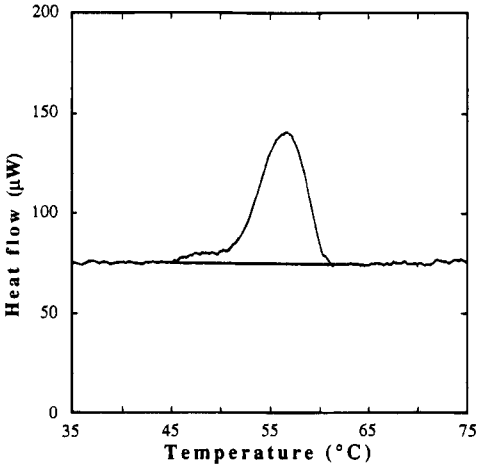

Figure 12. DSC cooling scan (0.5 deg/min; baseline subtracted) for DX (0.1% w/v in 10 mM KCl) in the presence of 0.2% w/v KM.

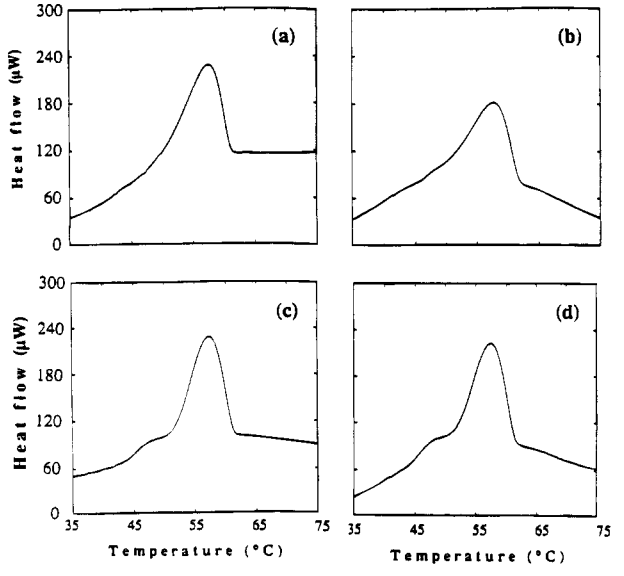

Figure 13. DSC cooling scans (0.5 deg/min) for DX (0.4% w/v in 10 mM KCl) in the presence of KM at concentrations (% w/v) of (a) 0.24, (b) 0.40, (c) 0.72, and (d) 1.00.

obtained for the same concentration of DX alone (0.1% w/v in 10 mM KCl). The spectra show the frequency (ω) dependence of the storage modulus (G'), loss modulus (G''), and complex dynamic viscosity ($\eta^* = \{G''^2 + G''^2\}^{1/2}/\omega$). For DX alone at this very low concentration, G' and G'' have comparable values over most of the accessible frequency range (0.1−100 rad s^{-1}), but log η^* shows a virtually linear dependence on log ω, which is one of the characteristic features of gel-like response.[18] Incorporation of small amounts of KM gives a significant enhancement in G', particularly at low frequencies. As the concentration of KM approaches that of DX, the spectra became typical of true gels (Figure 14c): elastic response (G') grossly exceeds viscous flow (G''), log η^* has a linear dependence on log ω with a slope close to −1, and G' is virtually independent of frequency. At higher concentrations of KM, however, the gel-like character decreases (Figure 14d): the slope of log η^* *vs* log ω and the separation between G' and G'' are reduced, and the moduli show a greater frequency dependence.

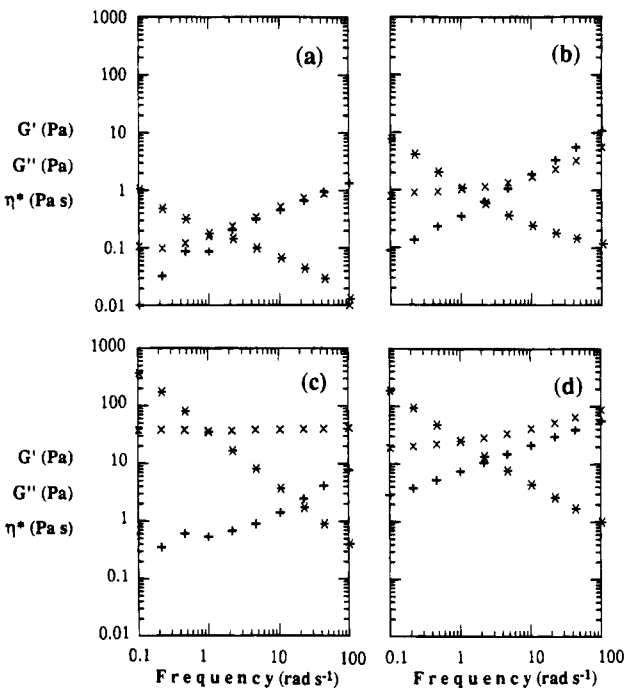

Figure 14. Mechanical spectra (10 °C; 2% strain) showing the frequency dependence of G' (×), G'' (+), and η^* (∗) for DX (0.1% w/v in 10 mM KCl) in combination with KM at concentrations (% w/v) of (a) 0.00 (i.e., DX alone), (b) 0.01, (c) 0.06, and (d) 0.60.

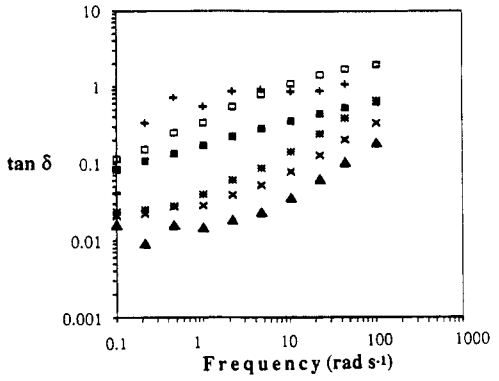

Figure 15. Frequency dependence of tan δ (10 °C; 2% strain) for DX (0.1% w/v in 10 mM KCl) alone (+) and in the presence of KM at concentrations (% w/v) of 0.01 (□), 0.03 (*), 0.06 (▲), 0.10 (×), and 0.40 (■).

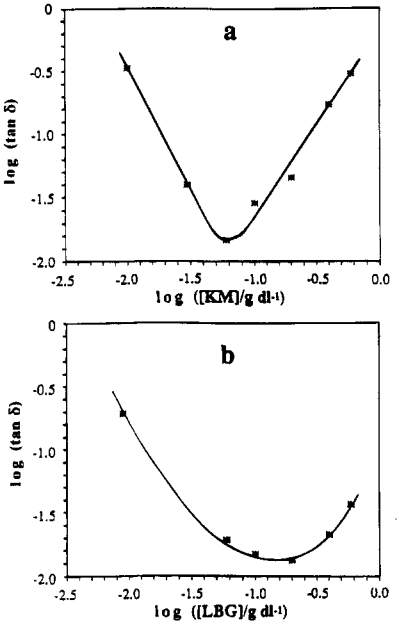

Figure 16. Variation of tan δ (1 rad s^{-1}; 2% strain; 10 °C) with concentration of (a) KM and (b) LBG in mixed gels with DX (0.1% w/v in 10 mM KCl).

The variation in the relative contributions of liquid-like and solid-like response with increasing concentration of KM is demonstrated directly in Figure 15, which shows the frequency dependence of tan δ (i.e., G''/G') for mixtures spanning the range of compositions studied. The initial reduction and subsequent increase in liquid-like character is clear. The composition dependence at fixed frequency is shown in Figure 16a, as a double-logarithmic plot of tan δ versus concentration of KM (with DX concentration held constant at 0.1% w/v in 10 mM KCl). The frequency used for the comparison was 1 rad s^{-1}, chosen as high enough to avoid the experimental scatter evident (Figure 14) at very low frequency but low enough to minimize contributions to overall rheological response from entanglement coupling of disordered KM chains. There is about a 30-fold variation in tan δ across the composition range studied, with a sharp minimum at a KM concentration of ~0.07% w/v (i.e., at KM/DX ≈ 0.7).

The origin of this behavior can be traced to the composition dependence of the individual moduli (Figures 9 and 10). Addition of low concentrations of KM causes a sharp increase in G' (Figure 8) but has little effect (Figure 9b) on the absolute values of G'', giving a drop in tan δ. (It should be noted that the traces shown

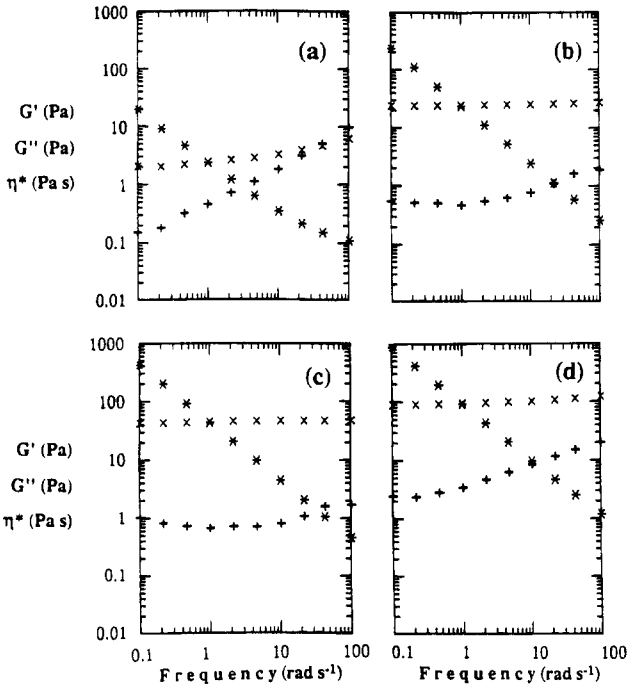

Figure 17. Mechanical spectra (10 °C; 2% strain) showing the frequency dependence of G' (×), G'' (+), and η^* (*) for DX (0.1% w/v in 10 mM KCl) in combination with LBG at concentrations (% w/v) of (a) 0.01, (b) 0.06, (c) 0.10, and (d) 0.60.

in Figure 9b for the two lowest concentrations of KM have been displaced downward by 1 decade, to avoid overlap with those for the next two concentrations in the series studied.) At higher concentrations of KM, by contrast, G' remains virtually constant (Figure 10) but G'' increases steadily, giving a corresponding increase in tan δ. The obvious interpretation is that at KM/DX ratios up to ~0.7 the KM associates with the DX to form a gel network, with consequent increase in G'; any additional KM remains unbound, giving an increase in viscous response (G'') but with little contribution to G'. As would be expected from this interpretation, the magnitude of the sharp rise in G'' at the gel point (Figure 9b) increases steadily with initial increase in KM concentration and then remains constant at higher concentrations.

An identical series of experiments was carried out using LBG in place of KM. The concentration of deacetylated xanthan was again held constant at 0.1% w/v in 10 mM KCl and the concentration of LBG was varied between 0.01 and 0.60% w/v. As found for KM, the gel-like character of the mixed systems after cooling to low temperature showed an initial increase and subsequent decrease with increasing content of LBG (Figure 17). Figure 16b shows tan δ at fixed frequency (1 rad s^{-1}) plotted double logarithmically against galactomannan concentration. The minimum in liquid-like character is less sharp than in the corresponding plot for KM (Figure 16a) and is displaced to higher concentration (~0.15% w/v, in comparison with ~0.07% for KM). As shown in Figure 10, further addition of LBG above ~0.15% w/v has little effect on G', and the absolute values of G' in this composition range are about 3 times higher than those obtained with KM.

Figure 18 shows the temperature dependence of G', G'', and tan δ for some representative DX/LBG mixtures. Values recorded on cooling and reheating were again closely superimposable. The gelation process

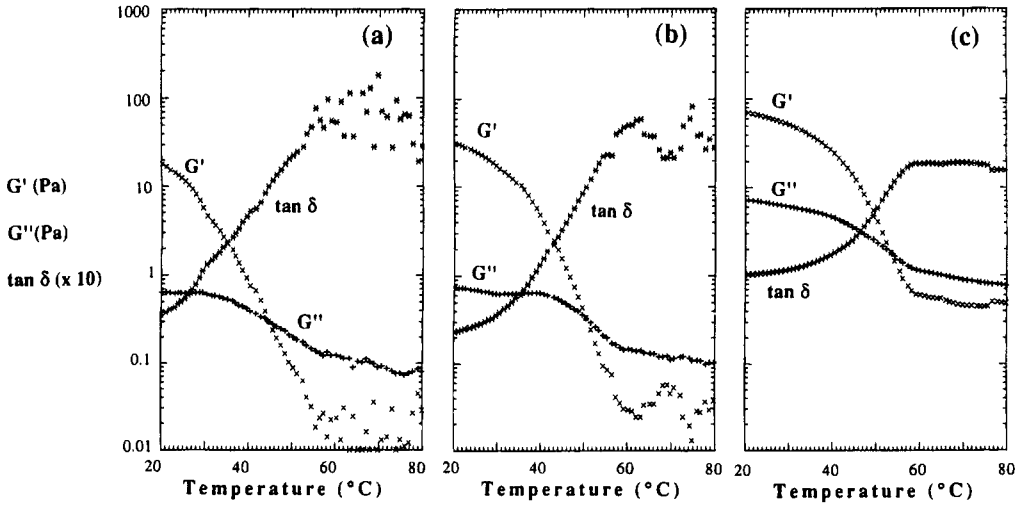

Figure 18. Temperature dependence of G', G'', and tan δ (10 rad s^{-1}; 2% strain) for DX (0.1% w/v in 10 mM KCl) in combination with LBG at concentrations (% w/v) of (a) 0.03, (b) 0.10, and (c) 0.60.

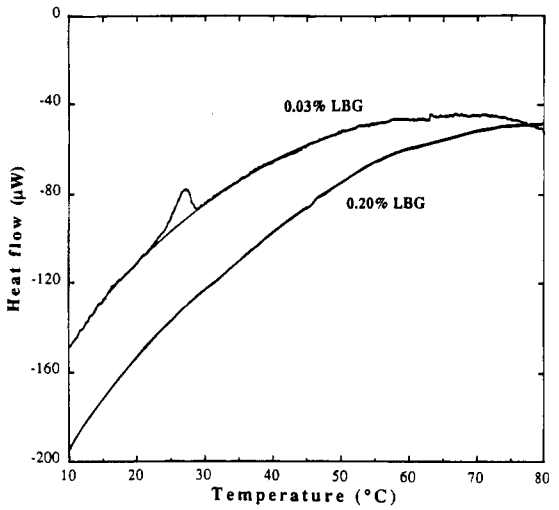

Figure 19. DSC cooling scans (0.5 deg/min) for DX (0.1% w/v in 10 mM KCl) in the presence of LBG at the concentrations shown.

spans a much wider temperature range than in the corresponding plots for DX/KM mixtures (Figure 9) but begins at the same point ($T_g \approx 60$ °C). There is perhaps a slight indication of a maximum in G'' when the two polymers are present in equal amounts (i.e., at 0.10% w/v LBG), but it is totally absent at higher or lower concentrations and far less evident than in corresponding plots for DX/KM (Figure 11). There was also no indication of a shoulder in the temperature dependence of tan δ for any of the DX/LBG mixtures studied.

As illustrated in Figure 19, DSC traces for DX/LBG mixtures with the LBG component present in excess were totally featureless, with no indications of thermal transitions either at the gel point or over the temperature range of conformational ordering for DX alone under the same ionic conditions ($T_m \approx 39$ °C; Figure 7). At lower concentrations of LBG, where the DX component is present in excess, there is again no evidence of a thermal transition associated with gel formation, in contrast to the large enthalpy changes observed (Figures 3 and 7) for xanthan or deacetylated xanthan in combination with KM. A small peak is, however, evident at lower temperature ($T_m \approx 27$ °C). It would seem reasonable to assume that this corresponds to the disorder–order transition of surplus DX. The midpoint temperature, however, is about 12 °C lower than that observed for DX alone under the same conditions. One possible explanation is that attachment of LBG to the xanthan molecule leaves short sequences of uncomplexed material, which therefore order at lower temperature than long chains. If this interpretation is correct, a similar low-temperature transition would also be expected for mixtures of DX with low concentrations of KM. No such transitions were observed. However, at the machine settings required to accommodate the intense thermal changes accompanying formation and melting of DX/KM gels, a peak of comparable size to that shown in Figure 19 would be difficult, or impossible, to resolve from the baseline.

Xanthan in 10 mM KCl ($T_m \approx T_g$). In the final series of experiments in this investigation, the ionic environment was again held constant at 10 mM KCl, but unmodified xanthan was used in place of DX (giving a higher value of T_m for the disorder–order transition of the xanthan component in isolation).

Figure 20 shows the temperature dependence of G', G'', and tan δ for a mixture of xanthan (0.32% w/v) and KM (0.24% w/v) under these ionic conditions. As in all the studies reported so far, the results obtained on reheating to melt the gel are virtually identical to those recorded on initial cooling from the high-temperature solution state. There are, however, two striking differences. The steep increase in G' on cooling begins at higher temperature (~67 °C, in comparison with $T_g \approx$ 60 °C for the other systems studied) and occurs in two distinct steps rather than as a single process. As found for KM in combination with DX under the same conditions of concentration and ionic environment (Figure 4), there is a broad maximum in the temperature course of G'', with an associated shoulder in tan δ. In this case, however, the form of the variation in tan δ will be influenced by the double rise in G', making detailed interpretation difficult.

Similar experiments were carried out using different concentrations of xanthan, but holding the KM concentration constant at 0.24% w/v. The temperature dependence of G' and G'' for these systems is shown in Figure 21. The maximum in G'' becomes broader as the xanthan concentration is increased and disappears at low concentration. In all cases, the steep rise in G' occurs in two steps and begins well above 60 °C.

The likely origin of the temperature-dependent changes in G' is demonstrated in Figure 22, which shows the variation in G' for a mixture of xanthan (0.32% w/v) and

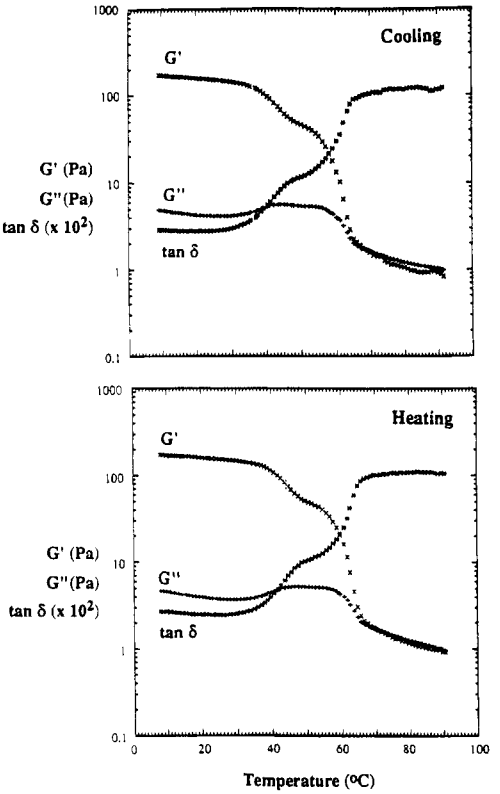

Figure 20. Variation of G', G'', and tan δ (10 rad s^{-1}; 2% strain) on cooling (upper curves) and reheating (lower curves) for xanthan (0.32% w/v in 10 mM KCl) in combination with KM (0.24% w/v).

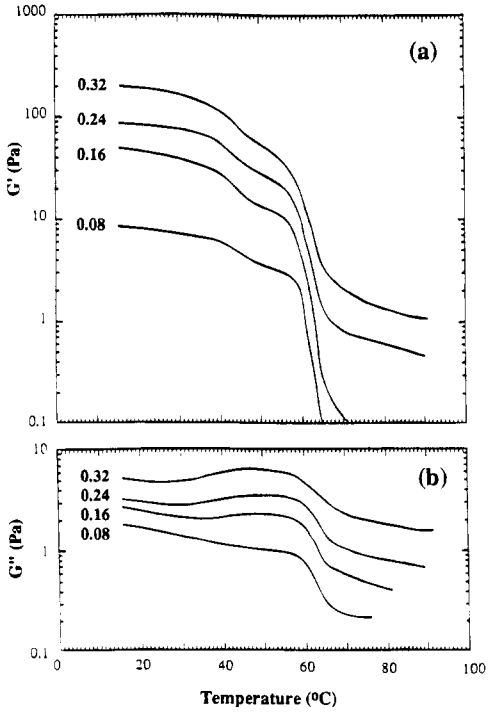

Figure 21. Temperature dependence of (a) G' and (b) G'' (10 rad s^{-1}; 2% strain) for KM (0.24% w/v in 10 mM KCl) in combination with xanthan at the concentrations (% w/v) shown beside the individual traces.

KM (0.24% w/v) in 10 mM KCl, in direct comparison with the values obtained using DX in place of xanthan, and with the temperature course of the disorder–order transition for xanthan alone under the same conditions (as monitored by DSC). The first increase in G' for the xanthan/KM system spans the same temperature range

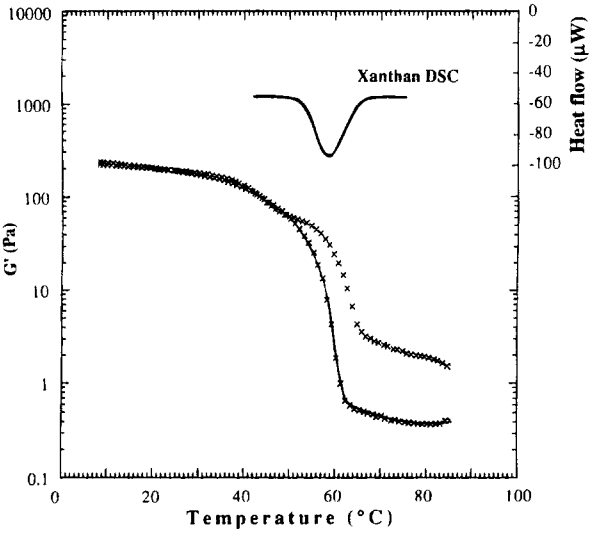

Figure 22. Lower traces: temperature dependence of G' (10 rad s^{-1}; 2% strain) for KM (0.24% w/v in 10 mM KCl) in the presence of 0.32% w/v xanthan (symbols only) or DX (solid line). Upper trace: DSC heating scan (0.2 deg/min) for xanthan alone (0.32% w/v in 10 mM KCl).

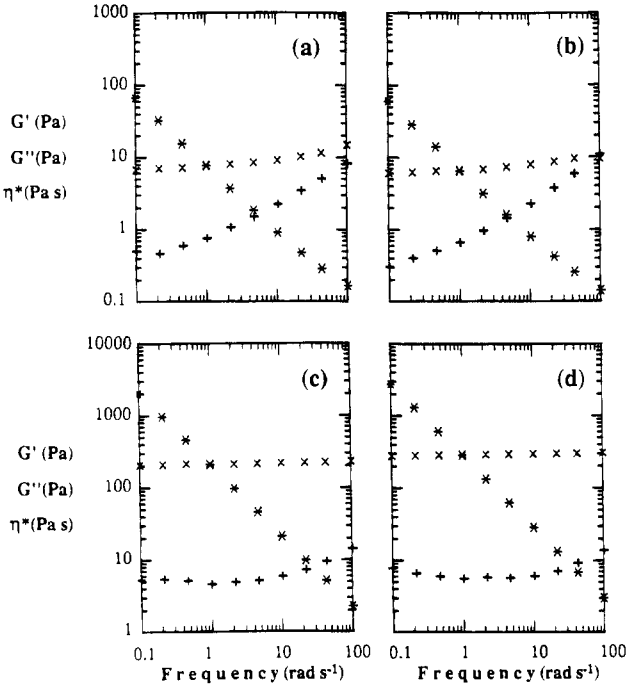

Figure 23. Mechanical spectra (10 °C; 2% strain) for KM (0.24% w/v in 10 mM KCl) in the presence of (a) 0.08% xanthan, (b) 0.08% DX, (c) 0.32% xanthan, and (d) 0.32% DX.

as the DSC transition for conformational ordering of xanthan alone; the second coincides closely with the temperature course of gelation for DX/KM. It therefore seems reasonable to conclude that the true onset of gelation occurs at ~60 °C, as in the other systems studied (DX/KM, DX/LBG, and xanthan/KM at higher salt), but is masked by overlap with the disorder–order transition for the xanthan component under the ionic conditions used (10 mM KCl).

Figure 23 shows mechanical spectra recorded on completion of the cooling scans in Figure 22, and for the same concentration of KM (0.24% w/v in 10 mM KCl) in the presence of a lower concentration of xanthan or DX (0.08% w/v). In both cases the spectra obtained for the xanthan/KM and DX/KM mixtures are virtually identical, indicating that acetate substituents on the

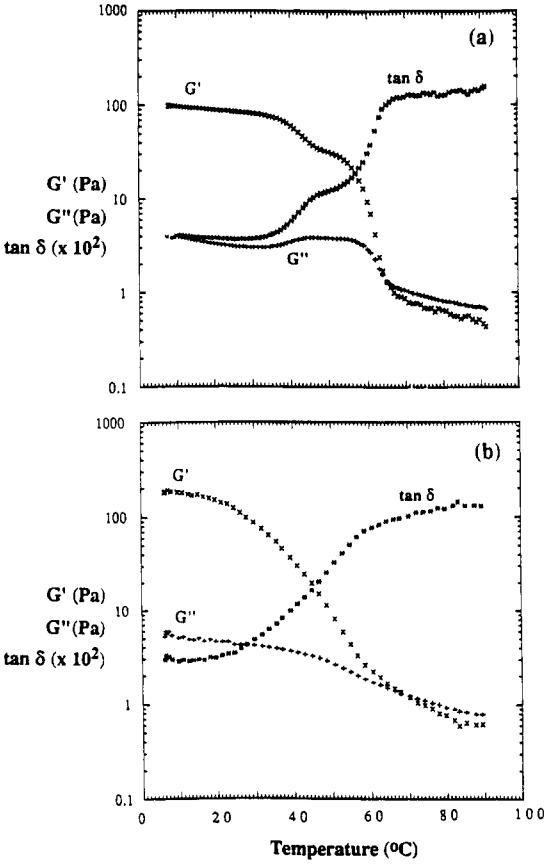

Figure 24. Temperature dependence of G', G'', and tan δ (10 rad s^{-1}; 2% strain) for xanthan (0.24% w/v in 10 mM KCl) in the presence of (a) KM or (b) LBG at 0.24% w/v.

xanthan component have no significant effect on the small-deformation mechanical properties of the mixed gels formed with KM under the conditions used in the present investigation.

Figure 24 illustrates the effect of replacing KM by LBG in mixed systems with xanthan in 10 mM KCl. The maximum in the temperature course of G'' and the accompanying shoulder in tan δ seen for mixtures incorporating KM are absent, as was also found for DX/LBG (Figure 18). The steep increase in G' on cooling again starts at ~67 °C (consistent with initial ordering of xanthan) but is much broader and shows no evidence of the involvement of two separate processes. The likely interpretation is that, as found for deacetylated xanthan, gelation with LBG occurs over a much wider temperature range than with KM, so that the sol–gel transition can no longer be resolved from the disorder–order transition at higher temperature.

Quantitative Analysis of DSC Results. As illustrated in Figures 3 and 7, gelation of xanthan or DX with KM is accompanied by a sharp exotherm in DSC (with a corresponding endotherm on heating). No such thermal processes were observed for mixed systems incorporating LBG in place of KM. However, since the sol–gel transitions for these systems are very broad, it is possible that corresponding thermal transitions are, in fact, present but are too wide to be resolved from the baseline in DSC.

The midpoint temperature of DSC peaks recorded at fixed scan rate for xanthan/KM or DX/KM mixtures shows no dependence on composition but, as illustrated in Figure 25, the apparent values of T_m on heating are higher than those obtained on cooling. The separation, however, decreases with decreasing scan rate (Figure

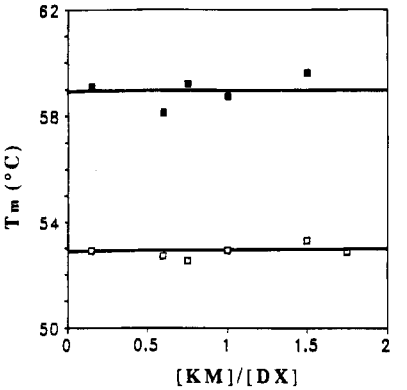

Figure 25. Midpoint temperatures for the thermal changes accompanying formation and melting of mixed gels of KM and DX in 10 mM KCl, from DSC cooling (□) and heating (■) scans at 0.5 deg/min. The values shown were obtained for DX concentrations ranging from 0.08 to 0.40% w/v and KM concentrations ranging from 0.06 to 1.0% w/v.

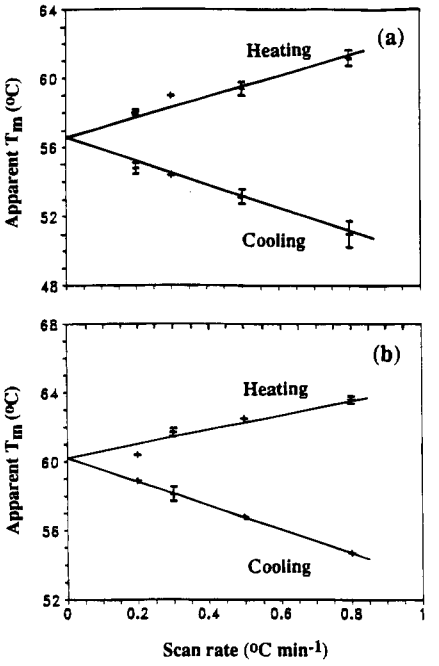

Figure 26. Scan-rate dependence of apparent T_m values from DSC heating and cooling scans for mixtures of KM (in 10 mM KCl) with (a) DX or (b) xanthan. The error bars show the standard deviation of values obtained at fixed scan rate for different compositions (cf. Figure 25).

26), with results from heating and cooling scans showing satisfactory convergence to a common intercept at zero scan rate, as would be anticipated from the absence of detectable thermal hysteresis between the gelation and melting processes monitored rheologically (e.g., Figure 20).

The intercept obtained (Figure 26b) for mixtures of xanthan and KM in 10 mM KCl is higher than the corresponding value for DX/KM (Figure 26a). This is consistent with the temperature dependence of G' (Figure 22) and, as discussed previously, can be attributed to the sol–gel transition overlapping with the disorder–order transition of xanthan at slightly higher temperature.

The enthalpy changes (ΔH) accompanying gelation of xanthan or DX with KM in 10 mM KCl at all polymer concentrations studied are listed in Table 1. Low-temperature shoulders, where present (e.g., Figures 12 and 13), were included in calculation of peak area.

Table 1. Enthalpy Changes (ΔH)[a] Accompanying Gelation of Xanthan (XAN) or Deacetylated Xanthan (DX) with Konjac Glucomannan (KM)

deacetylated xanthan				unmodified xanthan			
concentration[b]				concentration[b]			
KM	DX	KM/DX	ΔH	KM	XAN	KM/XAN	ΔH
0.24	0.32	0.75	24.2	0.24	0.32	0.75	9.9
0.24	0.24	1.00	25.0	0.24	0.24	1.00	12.1
0.24	0.16	1.50	29.9	0.24	0.16	1.50	19.6
0.24	0.08	3.00	27.8	0.24	0.08	3.00	22.3
0.24	0.04	6.00	29.0				
0.01	0.10	0.10	2.6	0.025	0.10	0.25	3.0
0.03	0.10	0.30	7.2	0.075	0.10	0.75	7.0
0.06	0.10	0.60	13.1	0.10	0.10	1.00	10.0
0.10	0.10	1.00	26.7	0.20	0.10	2.00	20.5
0.20	0.10	2.00	28.5	0.60	0.10	6.00	22.4
0.40	0.10	4.00	30.9	1.00	0.10	10.0	19.8
0.60	0.10	6.00	30.1				
0.04	0.40	0.10	4.7	0.60	0.40	1.50	17.8
0.06	0.40	0.15	5.1				
0.12	0.40	0.30	9.7				
0.24	0.40	0.60	20.5				
0.40	0.40	1.00	24.4				
0.70	0.40	1.75	29.3				
1.00	0.40	2.50	30.6				

[a] ΔH is expressed in joules per gram of xanthan or deacetylated xanthan. [b] Polymer concentrations are in g dL^{-1} (% w/v in 10 mM KCl).

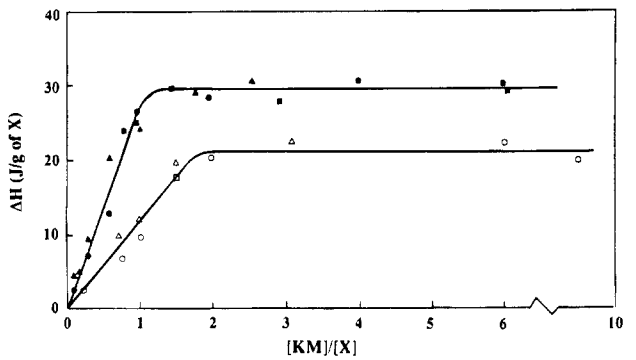

Figure 27. Composition dependence of thermal changes accompanying the sol–gel transition for mixtures of KM with xanthan (open symbols) or DX (filled symbols) in 10 mM KCl. [X] denotes the concentration (% w/v) of the xanthan or DX component and [KM] the concentration of the glucomannan. Heat changes (ΔH) are expressed relative to [X] alone (i.e., as joules per gram of xanthan or DX). Circles: [X] = 0.1% w/v, with varying [KM]; triangles: [X] = 0.4% w/v, with varying [KM]; squares: [KM] = 0.24% w/v, with varying [X].

Baselines were interpolated using a polynomial fit to heat-flow values above and below the temperature range of the transition. As shown in Figure 27, ΔH per gram of DX increases linearly with increasing concentration of KM until the two polymers are present in roughly equal amounts and then remains constant (at ~29 J g^{-1}) on further addition of KM. The results are essentially independent of overall concentration at each ratio of KM:DX. Mixtures of KM with xanthan show a similar pattern of behavior, but the maximum value of ΔH is lower (~21 J g^{-1}) and the proportion of KM required to achieve this maximum is higher.

Discussion and Conclusions

The very large enthalpy changes accompanying formation and melting of mixed gels of KM with xanthan or DX are, in themselves, indicative of a binding process. It could, in principle, be argued that the transitions arise from homotypic interactions of glucomannan chains, driven by thermodynamic incompatibility with the xanthan component. However, KM samples in which self-association was induced by freezing and thawing (in 10 mM KCl, as used here) have been found[41] to give featureless DSC traces on heating from 5 to 95 °C. Similar featureless traces were obtained for LBG after freezing and thawing. More directly, the composition dependence of ΔH (Figure 27) shows all the hallmarks of a binding interaction rather than of an exclusion mechanism, with values rising to a maximum at a fixed ratio of the two components, irrespective of their total concentration. The sharp minimum in tan δ (Figure 16a) and the associated plateau in G' (Figure 10) when KM concentration is increased in the presence of a fixed concentration of DX are also directly indicative of a binding process.

KM appears to form stronger associations with deacetylated xanthan than it does with the unmodified polymer. The maximum values of ΔH (Figure 27) are higher and are attained at a lower relative concentration of KM, suggesting that DX can bind to glucomannan sequences that are too short to form stable associations with unmodified xanthan. Studies of viscous interactions in very dilute solution[42] also indicate that binding of xanthan to KM (or to LBG) is enhanced by deacetylation, and it has been concluded from multivariant analysis of gel moduli that acetyl substituents on xanthan inhibit interaction with galactomannan chains.[43] As shown in Figure 23, however, mixed gels of KM with xanthan or with DX under otherwise identical conditions gave virtually identical mechanical spectra, indicating that while deacetylation may increase the strength of interaction, it does not affect the number of heterotypic junctions formed.

Sol–gel transitions for xanthan or deacetylated xanthan with LBG are much broader (i.e., less cooperative) than those observed with KM. As shown in Figure 10, however, the resulting gels are stronger (i.e., higher G'). Both observations are consistent with LBG having a larger number of shorter binding sites than KM. DSC scans for the mixed systems incorporating LBG (Figure 19) show no evidence of the intense heat changes seen with KM (e.g., Figure 7). Very broad exotherms spanning the temperature range of the sol–gel transition have, however, been observed[45] for more concentrated mixtures of xanthan and LBG (1% w/v of each component). It therefore seems likely that correspondingly thermal processes do indeed occur at the much lower concentrations used in the present work but are undetectable by DSC because of the width of the transition.

As discussed above, analysis of the composition dependence of ΔH (Figure 27) argues conclusively for heterotypic binding of KM. In the absence of discernible thermal transitions when KM is replaced by LBG, the most direct evidence of binding is the minimum in tan δ (Figure 17) and plateau in G' (Figure 10) observed on increasing LBG concentration at fixed concentration of DX. There is also an obvious "family relationship" in the synergistic behavior of KM and LBG, indicating a similar mechanism of interaction in both cases. In particular, the onset of synergistic gelation occurs at the same temperature for both.

The gelation temperature is also unaffected by the conformational state of the xanthan component. Gelation of KM with xanthan in 30 mM KCl begins (Figure 3) at ~60 °C, well below the temperature range of the disorder–order transition for xanthan alone under the

same ionic conditions ($T_m \approx 73$ °C). With deacetylated xanthan in 10 mM KCl, gelation also begins at ~60 °C (Figures 5 and 18), which is now well above the temperature range of conformational ordering ($T_m \approx 39$ °C; Figure 7). As discussed previously, this behavior is inconsistent with both the "Unilever" and "Norwich" models of synergistic interaction. It could of course be argued, in an extension of the "Unilever" model, that even at temperatures well above T_m there will be a very small, but finite, proportion of 5-fold order and that this will bind to mannan or glucomannan chains, continually pulling over the disorder–order transition until full ordering and association is attained. Conversely, it can be argued that, in terms of the "Norwich" model, a small fraction of disordered sequences could act as a reaction intermediate at temperatures well below T_m. There is, however, no reason to invoke the necessary involvement of structures present at vanishingly low concentrations. Under conditions where heterotypic junctions have lower free energy than competing states of molecular organization, their adoption (Figure 2c) is to be expected, irrespective of the conformational preferences of the xanthan component in the absence of cosynergist (although the rate of association could, of course, be limited by activation-energy barriers in the reaction pathway).

If mixing is carried out at a temperature substantially below T_g, the network is disrupted as it forms. Heating to above T_g and recooling gives a continuous gel. Comparison of the mechanical properties of mixtures prepared at, or heated to, different temperatures indicates[40,44] that it is this "annealing" process, rather than disordering of xanthan, which causes the increase in cohesiveness when samples mixed at room temperature are heated and cooled.

Evidence of the nature of the heterotypic structures has come entirely from the X-ray diffraction studies of the Norwich group. Their initial proposal[31] envisaged ordered assemblies with xanthan and galactomannan chains both present in the 2_1 conformation, and it was argued[32] that this would provide a complementary fit absent in the "Unilever" model. However, it should be noted that, in principle, there is no reason why galactomannan or glucomannan chains should not adopt a conformation with a pitch to match that of the cellulose backbone in the xanthan 5-fold helix. The ability of xanthan chains to adopt the 2-fold conformation (in which the trisaccharide side chains are clustered together along one side of the backbone) is less obvious. Computer modeling by Perez and Vergelati[46] indicated that arrangements of this type are blocked by steric clashes between the side chains. In a subsequent reexamination, however, Millane and Wang[47] concluded that a 2_1 structure could be formed if the pitch was extended to give a projected residue length of ~0.526 nm along the axis of symmetry, in comparison with 0.520 nm for cellulose[25] or mannan[23] and 0.470 nm for the xanthan 5-fold helix.[12]

The meridional reflections attributed to heterotypic junctions in mixed specimens of xanthan with LBG or tara gum were reported[32] to correspond to a residue rise of 0.52 nm, as was also observed for the galactomannans alone. The difference from the more extended conformation modeled by Millane and Wang may, however, be within the error limits of the measurements. Oriented fibers prepared from mixed gels of xanthan with KM, by contrast, gave an entirely different diffraction pattern,[33] for which the simplest interpretation is a 6-fold structure with a pitch of 5.6 nm.[34] This corresponds to a rise per residue of 0.467 nm, virtually identical to that of the 5-fold helix structure of xanthan alone.

The X-ray diffraction evidence of differences between the final state of macromolecular organization in mixtures of xanthan with galactomannans or with glucomannan may explain some puzzling features in the results of the present investigation. As discussed previously, the onset of synergistic gelation occurs at the same temperature for LBG and KM. The samples incorporating KM, however, then show evidence of structural rearrangement at lower temperature (maxima in G''; shoulders in tan δ and in DSC). A possible interpretation is that closely similar heterotypic junctions with 2-fold chain geometry are formed initially in both cases (giving closely similar values of T_g), but that the junctions involving KM then reorganize to the more compact 6-fold arrangement characterized in the condensed phase. The driving force for the rearrangement may come from glucose residues in the xanthan backbone interacting more strongly with glucose residues in KM than with mannose residues in LBG. A further indication of subtle differences in binding mechanism for galactomannans and glucomannan is that addition of electrolytes has been found to decrease the gelation temperature of xanthan in combination with KM,[48] whereas with LBG as cosynergist the onset of gel formation remains close to 60 °C in the presence or absence of salt.[40,49]

Finally, all steps in the formation and melting of the synergistic gels of xanthan or DX with LBG or KM appear to occur as equilibrium processes, with no evidence of thermal hysteresis at any stage.

Acknowledgment. We thank Dr. I. T. Norton and Dr. T. J. Foster (Unilver Research), Dr. V. J. Morris (Institute of Food Research, Norwich), and Dr. I. C. M. Dea (Leatherhead Food R.A.) for helpful discussions. We also thank CONACYT (Mexico) and Unilever Research for studentship support to F.M.G.

References and Notes

(1) Pettitt, D. J. In *Food Hydrocolloids*; Glicksman, M., Ed.; CRC Press: Boca Raton, FL, 1982; Vol. 1, pp 127–149.
(2) Jansson, P. E.; Kenne, L.; Lindberg, B. *Carbohydr. Res.* **1975**, *45*, 275.
(3) Melton, L. D.; Mindt, L.; Rees, D. A.; Sanderson, G. R. *Carbohydr. Res.* **1976**, *46*, 245.
(4) Morris, E. R. In *Molecular Structure and Function of Food Carbohydrate*; Birch, G. G., Green, L. F., Eds.; Applied Science: London, 1973; pp 125–132.
(5) Holzwarth, G. *Biochemistry* **1976**, *15*, 4333.
(6) Morris, E. R.; Rees, D. A.; Young, G.; Walkinshaw, M. D.; Darke, A. *J. Mol. Biol.* **1977**, *110*, 1.
(7) Milas, M.; Rinaudo, M. *Carbohydr. Res.* **1979**, *76*, 189.
(8) Norton, I. T.; Goodall, D. M.; Frangou, S. A.; Morris, E. R.; Rees, D. A. *J. Mol. Biol.* **1984**, *175*, 371.
(9) Muller, G.; Anrhourrache, M.; Lecourtier, J.; Chauveteau, G. *Int. J. Biol. Macromol.* **1986**, *8*, 167.
(10) Milas, M.; Rinaudo, M. *Carbohydr. Res.* **1986**, *158*, 191.
(11) Smith, I. H.; Symes, K. C.; Lawson, C. J.; Morris, E. R. *Int. J. Biol. Macromol.* **1981**, *3*, 129.
(12) Moorhouse, R.; Walkinshaw, M. D.; Arnott, S. *Extracellular Microbial Polysaccharides*; ACS Symposium Series 45; American Chemical Society: Washington, DC, 1977; pp 90–100.
(13) Okuyama, K.; Arnott, S.; Moorhouse, R.; Wilkinshaw, M. D.; Atkins, E. D. T.; Wolf-Ullish, Ch. *Fiber Diffraction Methods*; ACS Symposium Series 141; American Chemical Society: Washington, DC, 1980; pp 411–427.
(14) Hacche, L. S.; Washington, G. E.; Brant, D. A. *Macromolecules* **1987**, *20*, 2179.
(15) Liu, W.; Norisuye, T. *Biopolymers* **1988**, *27*, 1641.

(16) Liu, W.; Sato, T.; Norisuye, T.; Fujita, H. *Carbohydr. Res.* **1987**, *160*, 267.
(17) Morris, E. R. *Int. Food Ingredients* **1991**, *1*, 32.
(18) Ross-Murphy, S. B. In *Biophysical Methods in Food Research*; Chan, H. W.-S., Ed.; SCI Critical Reports on Applied Chemistry; Blackwell: Oxford, 1984; pp 138–199.
(19) Richardson, R. K.; Ross-Murphy, S. B. *Int. J. Biol. Macromol.* **1987**, *9*, 257.
(20) Ross-Murphy, S. B.; Morris, V. J.; Morris, E. R. *Faraday Symp. Chem. Soc.* **1983**, *18*, 115.
(21) Milas, M.; Rinaudo, M.; Knipper, M.; Schuppiser, J. L. *Macromolecules* **1990**, *23*, 2506.
(22) Dea, I. C. M.; Morrison, A. *Adv. Carbohydr. Chem. Biochem.* **1975**, *31*, 241.
(23) Winter, W. T.; Song, B. K.; Bouckris, H. *Food Hydrocolloids* **1987**, *1*, 581.
(24) Millane, R. P.; Hendrixson, T. L.; Morris, V. J.; Cairns, P. In *Gums and Stabilisers for the Food Industry 6*; Phillips, G. O., Williams, P. A., Wedlock, D. J., Eds.; IRL Press: Oxford, 1992; pp 531–534.
(25) Sundararajan, P. R.; Marchessault, R. H. *Can. J. Chem.* **1972**, *50*, 792.
(26) Nishinari, K.; Williams, P. A.; Phillips, G. O. *Food Hydrocolloids* **1992**, *6*, 199.
(27) McCleary, B. V. *Carbohydr. Res.* **1979**, *71*, 205.
(28) Dea, I. C. M.; Clark, A. H.; McCleary, B. V. *Food Hydrocolloids* **1986**, *1*, 129.
(29) Dea, I. C. M.; Clark, A. H.; McCleary, B. V. *Carbohydr. Res.* **1986**, *147*, 275.
(30) Dea, I. C. M.; Morris, E. R.; Rees, D. A.; Welsh, E. J.; Barnes, H. A.; Price, J. *Carbohydr. Res.* **1977**, *57*, 249.
(31) Cairns, P.; Miles, M. J.; Morris, V. J. *Nature (London)* **1986**, *322*, 89.
(32) Cairns, P.; Miles, M. J.; Morris, V. J.; Brownsey, G. J. *Carbohydr. Res.* **1987**, *160*, 411.
(33) Brownsey, G. J.; Cairns, P.; Miles, M. J.; Morris, V. J. *Carbohydr. Res.* **1988**, *176*, 329.
(34) Morris, V. J. In *Gums and Stabilisers for the Food Industry 6*; Phillips, G. O., Williams, P. A., Wedlock, D. J., Eds.; IRL Press: Oxford, 1992; pp 161–171.
(35) Tako, M.; Nakamura, S. *Carbohydr. Res.* **1985**, *138*, 207.
(36) Tako, M. *Carbohydr. Polym.* **1991**, *16*, 239.
(37) Tolstoguzov, V. B. *Food Hydrocolloids* **1991**, *4*, 429.
(38) Kovacs, P. *Food Technol.* **1973**, *27*, 26.
(39) Cheetham, N. W. H.; McCleary, B. V.; Teng, G.; Lum, F.; Maryanto *Carbohydr. Polym.* **1986**, *6*, 257.
(40) Goycoolea, F. M.; Foster, T. J.; Richardson, R. K.; Morris, E. R.; Gidley, M. J. In *Gums and Stabilisers for the Food Industry 7*; Phillips, G. O., Williams, P. A., Wedlock, D. J., Eds.; IRL Press: Oxford, 1994; pp 333–344.
(41) Goycoolea, F. M. Rheology and Interactions of Plant Polysaccharides. Ph.D. Thesis, Cranfield University, Bedford, UK, 1994.
(42) Foster, T. J.; Morris, E. R. In *Gums and Stabilisers for the Food Industry 7*; Phillips, G. O., Williams, P. A., Wedlock, D. J., Eds.; IRL Press: Oxford, 1994; pp 281–289.
(43) Shatwell, K. P.; Sutherland, I. W.; Ross-Murphy, S. B.; Dea, I. C. M. *Carbohydr. Polym.* **1991**, *14*, 131.
(44) Morris, E. R.; Foster, T. J. *Carbohydr. Polym.* **1994**, *23*, 133.
(45) Williams, P. A.; Day, D. H.; Langdon, M. J.; Phillips, G. O.; Nishinari, K. *Food Hydrocolloids* **1991**, *4*, 489.
(46) Perez, S.; Vergelati, C. *Int. J. Biol. Macromol.* **1987**, *9*, 211.
(47) Millane, R. P.; Wang, B. *Carbohydr. Polym.* **1990**, *13*, 57.
(48) Annable, P.; Williams, P. A.; Nishinari, K. *Macromolecules* **1994**, *27*, 4204.
(49) Foster, T. J. Conformation and Properties of Xanthan Variants. Ph.D. Thesis; Cranfield Institute of Technology, Bedford, UK, 1992.

MA946414S